

## Ab Initio Study of Optoelectronic Properties of VSb<sub>2</sub> Compound

Siham Malki<sup>1</sup> and Larbi El Farh<sup>1\*</sup>

Physics Department, Faculty of Sciences, University of Mohammed 1<sup>st</sup>, Oujda, Morocco.

Received 17 June 2019, Revised 18 February 2020, Accepted 14 July 2020

### ABSTRACT

The optoelectronic properties of VSb<sub>2</sub> compound were studied using the Full Potential Linearized Augmented Plane Wave (FP-LAPW) method, in accordance with the Density Functional Theory (DFT). Thus, this study calculated the total (TDOS) and partial (PDOS) density of states by the Engel-Vosko Generalized Gradient Approximation (EV-GGA) implemented in the Wien2k code. From the calculations, the material possesses a metallic character. Furthermore, the calculation involves the energy range between 0 eV and 14 eV, the optical spectra including the real and imaginary part of the dielectric function, the refractive index, the extinction coefficient, the optical conductivity, the absorption coefficient, the reflectivity and the loss function, considering both intra- and inter-band transitions. The optoelectronic properties study of VSb<sub>2</sub> intermetallic compound is important because this material is likely to be used as a diffusion barrier, as an electrode or in photovoltaic cells after doping or association with other materials. The results of the electronic properties show the main contribution of the V-3d states in the DOS. Similarly, the total density of states at Fermi energy  $N(E_F)$  is 6.4 States/eV and an electron specific heat coefficient  $\gamma$  is 15.1 mJ.mol<sup>-1</sup>.K<sup>-2</sup>. As for the optical properties, the VSb<sub>2</sub> is found to have a strong absorbance in the ultraviolet region and high reflectance in the infrared domain. This work is original because, according to the literature, even if this material has already been synthesized, no experimental or theoretical calculation of the optical properties has been made until now.

**Keywords:** EV-GGA, FP-LAPW, Optoelectronic Properties, VSb<sub>2</sub> Compound.

### 1. INTRODUCTION

A single-phase sample of di-antimonide VSb<sub>2</sub> was first synthesized in 1951 by Nowotony *et al.* [1]. It was obtained from the powder of Sb and small pieces of vanadium mixed in stoichiometric ratio with an extra of 3 to 5 wt.% antimony to compensate for losses during heat treatment performed at 800°C [2]. The VSb<sub>2</sub> compound crystallizes in the tetragonal unit cell I4/mcm (space group no. 140) and lattice parameters are  $a = b = 6.5538 \text{ \AA}$  and  $c = 5.6366 \text{ \AA}$  [3]. Based on this information, some properties of this material such as structural, electronic and optical properties at zero temperature can be determined [4]. The thermoelectric properties can also be investigated with BoltzTraP program [5], which can be interfaced with the Wien2k code.

According to literature studies, VSb<sub>2</sub> compound was tested as anodic material [6] and as electrode or diffusion barriers for Sb-based skutterudites thermoelectric devices [2]. However, no study has been reported on its optical properties. Generally, the knowledge of the optical properties is important in order to improve battery performance [7]. Therefore, it is useful to report it in this work of an ab-initio calculation within density functional theory to determine these properties. The electronic study carried out from the density of states shows the importance of the contribution of the V-3d orbital compared to that of the Sb-5p orbital and the metallic character

\*Corresponding author: [l.elfarh@ump.ac.ma](mailto:l.elfarh@ump.ac.ma)

of VSb<sub>2</sub> compound. This last property is confirmed by optical studies which are considered an important research topic for industrial applications as well as in fundamental research. Indeed, the optical properties are of paramount importance because they allow studying the interaction between the light (in the different domains visible, ultraviolet, and infrared) and the matter. Several works have been carried out in this direction [8-10].

VSb<sub>2</sub> compound can be used as diffusion barriers or electrode for Sb-based skutterudite thermoelectric devices [2]. As it can be used as electrode batteries, since Yazami's works [11] have aimed at improving the performance of Lithium alloy anodes such as the binary antimonide VSb<sub>2</sub>, CrSb<sub>2</sub>, and TiSb<sub>2</sub>. Those materials are expected to spread not only over small mobile application but also in the Hybrid Electric Vehicles (HEV).

For determine the properties of VSb<sub>2</sub> compound, the FP-LAPW method which is considered one of the most precise schemes is used to solve the Kohn-Sham equations and to enable most accurate calculations of the crystal properties on the atomic scale [12].

## 2. COMPUTATIONAL DETAILS

The calculations are carried out using the full-potential linearized augmented plane-wave (FP-LAPW) method in the framework of Density Functional Theory (DFT) as implemented in the WIEN2K code [13], whose the procedure of solving the self-consistent Kohn-Sham equation is given in Figure 1.

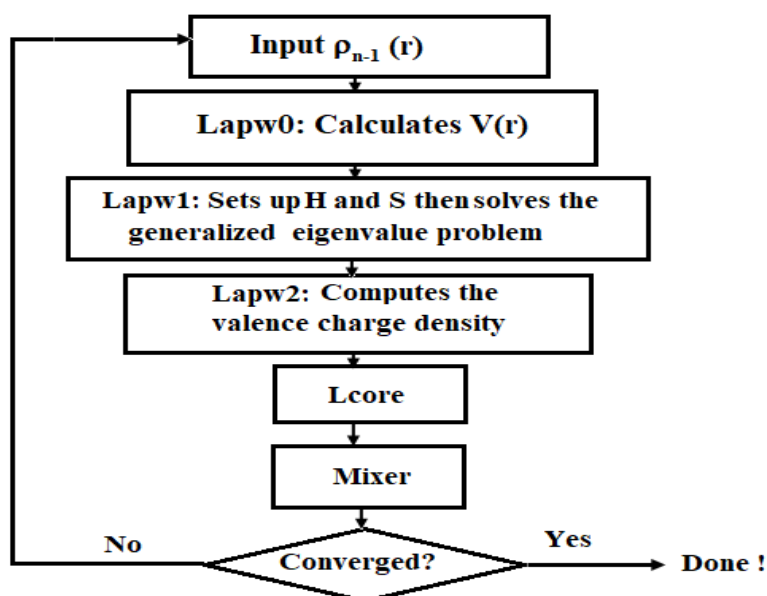


**Figure 1.** Flow chart of WIEN2k code [13], with H, S, V(r),  $\rho(r)$  are respectively Hamiltonian matrix, overlap matrix, potential, and electron density.

The optoelectronic properties of VSb<sub>2</sub> compound were calculated using the exchange-correlation functional called Engel-Vosko generalized gradient approximation (EV-GGA) [14]. The code parameters must be optimized to have a stable structure of the material to determine the different properties of the fundamental state. Thus, the product of  $RMT_{\min} * K_{\max} = 8.5$  (where  $RMT_{\min}$  is the smallest atomic sphere radius in a unit cell and  $K_{\max}$  is the maximum wave vector module in the first irreducible Brillouin zone) was obtained and a dense mesh of 800 k-points was used in the first Brillouin zone. Inside the atomic spheres, the maximum value of the angular

moment  $l_{\max}$  was set at 10 and the cut-off energy of core set at -6.0 Ry. The self-consistent calculations considered to converge when the total energy difference between successive iterations is less than 0.0001 Ry per formula unit. From these data, the electronic and optical properties of VSb<sub>2</sub> compound were calculated.

### 3. RESULTS AND DISCUSSION

#### 3.1 Electronic Properties

Figure 2 displays the calculated total and partial densities of states of VSb<sub>2</sub> compound. It shows that Fermi level  $E_F$  (dashed line) lies in a region of high DOS, thus revealing a metallic behaviour. This result has been confirmed by our calculation of the band structure using generalized gradient approximation (GGA) and modified Becke-Johnson (mBJ) potential scheme [15].

Calculations of electronic structure using TB-LMTO-ASA program package and measurements of the electrical resistivity as a function of the temperature carried out by Armbrüster *et al.* [16], confirmed the metallic character of VSb<sub>2</sub>.

Likewise, we note that the main contribution in the partial DOS plot is due to the 3D state of vanadium atom, involving easier electronic transitions to this state. While the contribution of 5p state of antimony atom is very weak.

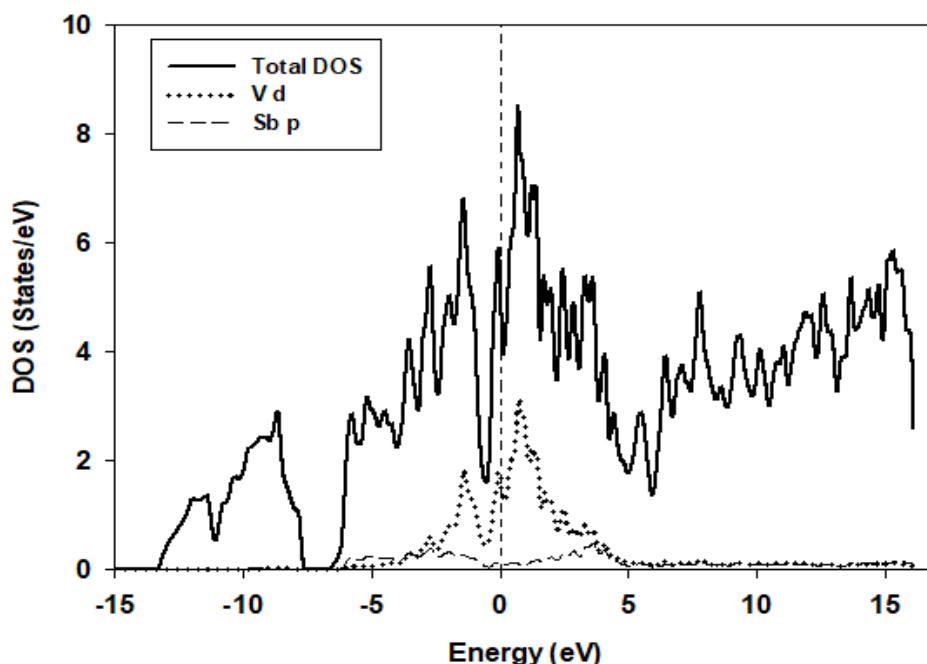


**Figure 2.** Total and partial densities of states of VSb<sub>2</sub> compound using EV-GGA.

From Figure 2, the total density of states at Fermi energy  $N(E_F)$  is approximately 6.4 States/eV. Armbrüster *et al.* [16] using Stuttgart TB-LMTO-ASA program employed the tight-binding (TB) version of the linear muffin-tin orbital (LMTO) [17] method in the atomic sphere approximation (ASA) found the total density approximately 7.2 States/eV. Meanwhile, in this study, the full-potential linearized augmented plane wave (FP-LAPW) method was used as implemented in the Wien2k code [18]. The difference in results is due to the use of two different methods.

Thus, the  $\gamma$  electron specific heat coefficient can be calculated using the following expression in Equation (1):

$$\gamma = \frac{N_A \pi^2 N(E_F) k_\beta^2}{3} \quad (1)$$

Where  $N_A$  is Avogadro's number and  $k_\beta$  is the Boltzmann's constant. Thus, the  $\gamma$  obtained is 15.1 mJ.mol<sup>-1</sup>.K<sup>-2</sup> for VSb<sub>2</sub>.

### 3.2 Optical properties

#### 3.2.1 The Dielectric Function

The dielectric function  $\varepsilon(\omega)$  is complex and can be expressed as in Equation (2) where  $\varepsilon_1(\omega)$  and  $\varepsilon_2(\omega)$  are the real and the imaginary part, respectively.

$$\varepsilon(\omega) = \varepsilon_1(\omega) + i\varepsilon_2(\omega) \quad (2)$$

It contains all intrinsic effects corresponding to the processes of light-matter interaction. In other words, it reflects the interaction of photons of radiation with the electrons of the material. Since VSb<sub>2</sub> has shown a metallic behaviour, in the expression of the dielectric function, two types of contributions have to be taken into account which are inter-band and intra-band. Therefore, the total dielectric function  $\varepsilon(\omega)$  is written as in Equation (3):

$$\varepsilon(\omega) = \varepsilon^{[intra]}(\omega) + \varepsilon^{[inter]}(\omega) \quad (3)$$

The intra-band transitions correspond to electronic conduction by free carriers. While the inter-band transitions are due to electron transitions from the occupied states below the Fermi level, to the unoccupied states in a higher band, caused by its absorption of electromagnetic radiation [19]. In other words, the last effect concerns bound electrons. The curves in Figure 3(a) and 3(b) represent the real and imaginary part of the dielectric function of VSb<sub>2</sub> respectively in the energy range [0; 14 eV].

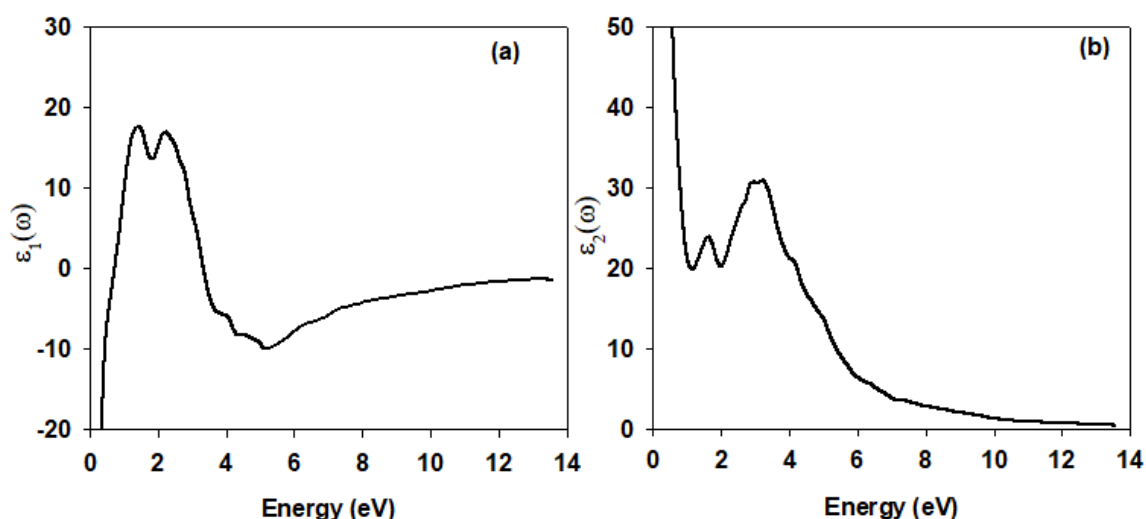


Figure 3. The real (a) and imaginary parts (b) of the dielectric function.

From the spectrum of the real part of the dielectric function in Figure 3(a), the large negative value of the real part of the dielectric function at low energies, which confirms the metallic character of VSb<sub>2</sub> compound. The first root of  $\varepsilon_1(\omega) = 0$  is at 0.7 eV, it is located in the near-infrared domain, where the optical response is dominated by the intra-band transition. This is due to the

oscillating of the charge carriers caused by the incident electromagnetic radiation [20]. This value corresponds to plasmonic oscillations. In order to obtain a better optical spectrum of the dielectric function, it is essential to sample the Brillouin zone as finely as possible [21], in this case, for VSb<sub>2</sub>, several points  $k = 800$  were taken.

Based on Figure 3(a), the real part  $\epsilon_1(\omega)$  of the dielectric function of VSb<sub>2</sub> takes negative values in the energy range 0 – 0.7 eV, with very low value when energy tends to 0. First, this highlights the mechanism of free electrons [22], and second confirms the metallic character of VSb<sub>2</sub>.  $\epsilon_1(\omega)$  is positive in the range 0.7 – 3.3 eV, with the occurrence of two highest peaks, one centred at 1.4 eV in the infrared range, and the other at 2.1 eV in the visible range. Indeed, they are both related to inter-band transitions of bonding electrons [23]. From 11.5 eV, notice that the real part of the dielectric function takes negligible values.

The imaginary part of dielectric function  $\epsilon_2(\omega)$  (refer Figure 3(b)) takes great positive values when energy tends to 0. Thus, the VSb<sub>2</sub> compound has a metallic behaviour which is in good agreement with the density of states calculation. In other words, a low energy incident photon allows electrons transmission in intra-band. But, at 0.7eV energy value, rapid decreases of the curve can be observed, which again implies plasmonic oscillation. By increasing the energy of the incident photons, the electronic transitions increase, hence, the first peak of electronic transition at 1.6 eV in the limit of near-infrared – visible, followed by the second peak at 3.3 eV located in the limit visible – near UV were observed. These two peaks are generally due to the optical transitions (inter-band transition) [22].

### 3.2.2 The refractive index

The complex refractive index  $n(\omega)$  consists of a real part  $\eta(\omega)$  (refractive index) and the imaginary part  $\kappa(\omega)$  (extinction coefficient) which shows the energy absorption of the incident wave by the material [24]. This property is given by the expression in Equation (4):

$$n(\omega) = \eta(\omega) + i\kappa(\omega) \quad (4)$$

Figure 4 presents the variation of refractive index and extinction coefficient as a function of energy  $\eta(\omega)$  and  $\kappa(\omega)$  respectively. For low energy,  $\eta$  takes great values owing to the presence of free electrons [22]. This is due to the metallic character of VSb<sub>2</sub> compound.

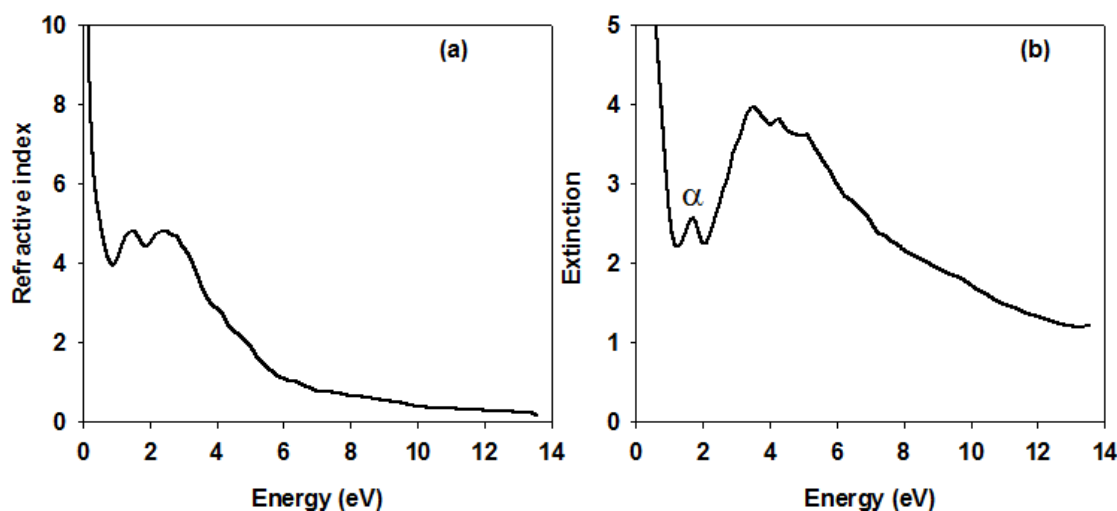


Figure 4. (a) Refractive index and (b) extinction coefficient of compound VSb<sub>2</sub>.

At the limit of near IR–visible, a broad peak appears, labelled by  $\alpha$  in Figure 4(b). However, for the high energy regime, greater than 6.3 eV; the refractive index is less than one, indicating possible super-luminescence phenomenon in the compound. This effect can be used in some applications such as optoelectronics devices, electronics, the optical communications, optical networks, and waveguides components [25-26]. This is corroborated by the decrease of the extinction index,  $\kappa$ , (Figure 4(b)). Generally, the peaks in  $\eta(\omega)$  and  $\kappa(\omega)$  spectra in the infrared region are due mainly to the intra-band transition of electrons.

### 3.2.3 The absorption coefficient

The absorption coefficient is given by the relation in Equation (5) where  $\kappa(\omega)$  is the extinction coefficient, and  $c$  the speed of light in a vacuum [27].

$$\alpha(\omega) = \frac{2\omega\kappa(\omega)}{c} \quad (5)$$

Figure 5 shows the evolution of the absorption coefficient of VSb<sub>2</sub> material as a function of incident energy in the range of 0 eV to 14 eV comprising infrared, visible and ultraviolet domains. Due to the metallic character of this compound, absorption starts at very low photon energy. In the visible domain, the absorption curve rises rapidly with the energy until reaching a maximum absorption value in the ultraviolet domain. Subsequently, absorption remains high due to the inter-band transitions [28]. Most of the light absorbed in infrared and visible spectra contributes to the electron transition [29] from the valence to conduction bands. From the absorption spectrum of VSb<sub>2</sub> which reaches a saturated limit in the middle-ultraviolet region, this compound is more absorbent in the ultraviolet region than in the infrared and visible regions.

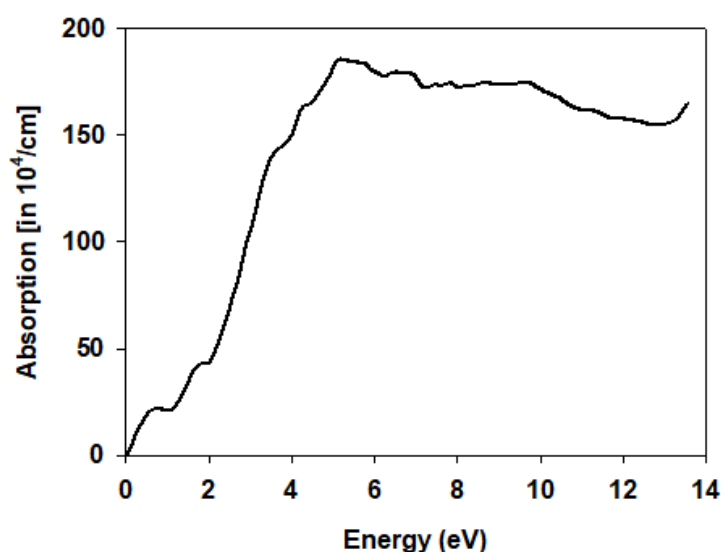
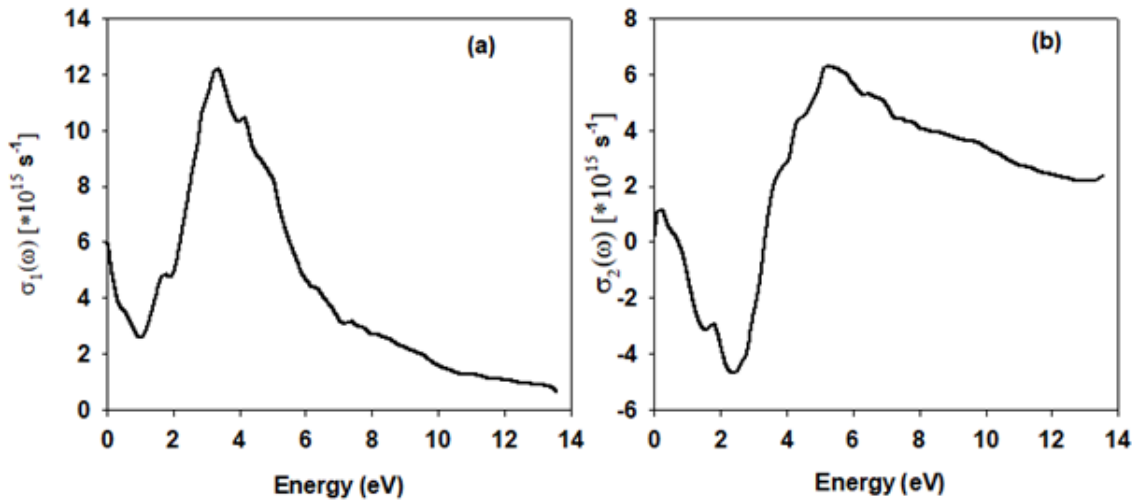


Figure 5. Absorption coefficient  $\alpha(\omega)$  of VSb<sub>2</sub> compound.

### 3.2.4 The optical conductivity

Another calculated optical parameter, depending on the intra- and inter-band transitions of electrons, is the optical conductivity  $\sigma(\omega)$ , consisting of a real part  $\sigma_1(\omega)$  (which defines the Ohmic losses) and an imaginary part  $\sigma_2(\omega)$  as in Equation (6) [30].

$$\sigma(\omega) = \sigma_1(\omega) + i\sigma_2(\omega) = -i\varepsilon_0\omega(\varepsilon(\omega) - 1) \quad (6)$$



**Figure 6.** The real and imaginary parts of the optical conductivity of VSb<sub>2</sub> compound.

Like all properties, the complex conductivity depends on the incident energy. The real part of conductivity begins at about  $5.3 \times 10^4 \text{ S.m}^{-1}$  for very low energy of a photon, which is in agreement with the band structure of the VSb<sub>2</sub> compound which does not show a bandgap [15].

In the infrared region, the conductivity decreases sharply to reach a minimum value of  $2.3 \times 10^4 \text{ S.m}^{-1}$  around 1 eV, then it increases to reach a maximum value of  $1.1 \times 10^5 \text{ S.m}^{-1}$  at 3.3 eV. This shows that the number of free charge carriers generated increases when the material absorbed an incident electromagnetic wave [31], especially in near-ultraviolet range, which is due generally to the inter-band transitions. In other words, the maximum of the spectrum of the conductivity usually corresponds to a maximum photo-current [24]. In the energy range where the optical conductivity is maximum, the compound behaves as a good conductor of when exposed to incident radiation. Beyond 3.3 eV, the real part of conductivity decreases with a rise in the frequency. In addition, the imaginary part of the conductivity is responsible for the phase shift between the local electric field and the current density [32].

For low frequencies, the imaginary part of the conductivity takes values smaller than the real part ( $\sigma_2 \ll \sigma_1$ ). In contrast, in the limit ultraviolet, the  $\sigma_2 \gg \sigma_1$ . Thus, the electrons have an inductive character [33].

### 3.2.5 The Reflectivity

The reflectivity  $R(\omega)$  can be defined as the ratio between the reflected flux and the flux incident by surface element. It is given by the following relation in Equation (7) where  $\varepsilon_1(\omega)$  and  $\varepsilon_2(\omega)$  are respectively the real and imaginary parts of the dielectric function.

$$R(\omega) = \frac{\left( (\varepsilon_1 + i\varepsilon_2)^2 - 1 \right)}{\left( (\varepsilon_1 + i\varepsilon_2)^2 + 1 \right)} \quad (7)$$

As shown in Figure 7, at very low energy, the reflectivity of VSb<sub>2</sub> compound is higher than 95%, which is reasonable if considering the metallic character of this compound. The reflectivity decreases rapidly in the infrared range to an absolute minimum of about 48% at about 1.2 eV. It increases to about 64% in visible and near ultraviolet domains and oscillate between 65% and 78% in the rest of the energy domain.

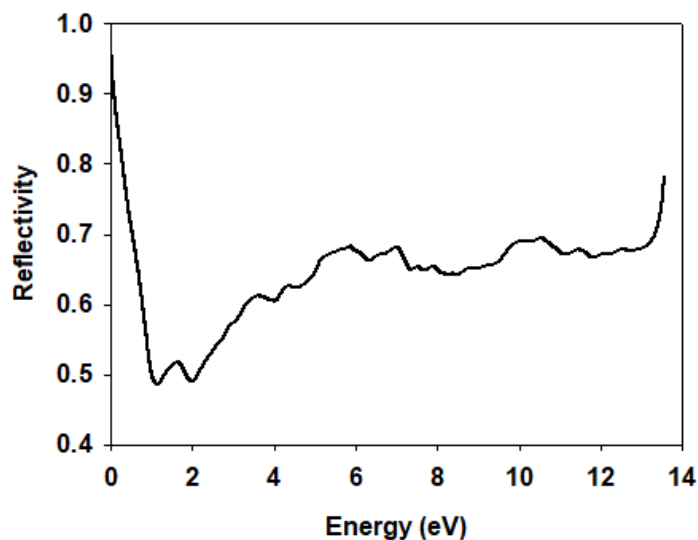


Figure 7. The reflectivity spectra of VSb<sub>2</sub> compound.

### 3.2.6 The Energy Loss Function

This property describes the loss of electronic energy when an electromagnetic wave transit through the material. It provides information about plasmon excitation, the inter-band and intra-band transitions [34]. The electron energy loss function  $L(\omega)$  is given by Equation (8):

$$L(\omega) = \frac{\varepsilon_2(\omega)}{\varepsilon_1^2(\omega) + \varepsilon_2^2(\omega)} \quad (8)$$

Figure 8 shows that in the range 0 – 0.7 eV, the energy loss function increases with increasing photon energy, this correspond to the negative value of  $\varepsilon_1(\omega)$  in this domain, revealing the loss of light transit for VSb<sub>2</sub> compound. In addition, the peak at 0.7 eV is related to plasma resonance and the corresponding energy is so-called plasma energy.

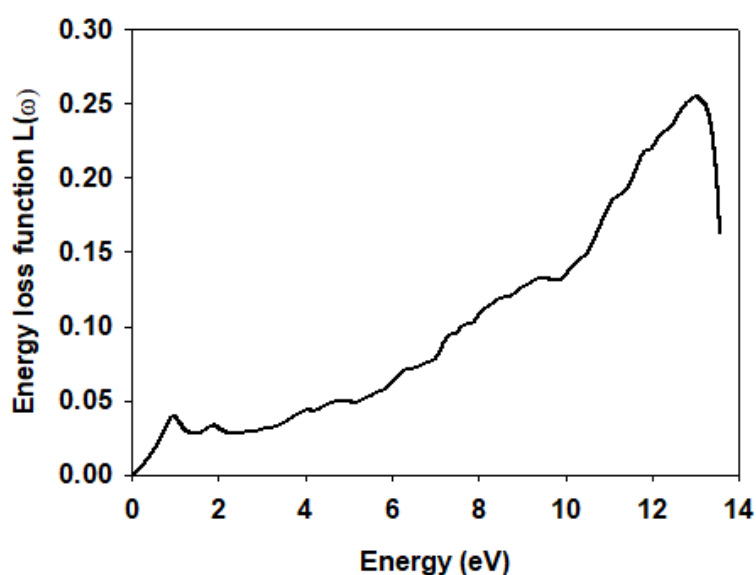


Figure 8. The energy loss function of VSb<sub>2</sub> compound.



#### 4. CONCLUSION

Based on the (FP-LAPW) method under Density Functional Theory (DFT) in Wien2k code with Engel-Vosko Generalized Gradient Approximation (EV-GGA), the density of states (DOS) and the optical properties of VSb<sub>2</sub> compound were studied. From the density of states at the Fermi level, the electronic specific heat coefficient  $\gamma$  can be deduced which is found to be 15.1 mJ.mol<sup>-1</sup>.K<sup>-2</sup>. This small value means that electronic contributions dominate the thermal conductivity.

The calculations of the density of states show an overlap between the conduction band and the valence band this indicates that VSb<sub>2</sub> material is a metal.

The optical properties versus incident energy such as the dielectric function  $\epsilon(\omega)$ , optical conductivity  $\sigma(\omega)$ , refractive index  $n(\omega)$ , absorption coefficient  $\alpha(\omega)$ , loss function  $L(\omega)$  and reflectivity  $R(\omega)$ , within the range [0; 14eV] were calculated and discussed. The intra-band and inter-band transitions were considered. Thus, the results confirm the metallic character of the studied compound VSb<sub>2</sub>. Indeed, at low energy, large negative values of  $\epsilon_1(\omega)$  and large positive values of  $\epsilon_2(\omega)$  were obtained. The refractive index takes a maximum value and the reflectivity is higher than 95% due to free electrons, and the observed peak in the electron energy loss spectrum corresponds to the plasma frequency.

Finally, the optical properties of VSb<sub>2</sub> compound are very interesting in the ultraviolet region. The objective of this work was to understand the optical properties of the VSb<sub>2</sub> compound, which have not been investigated so far by ab-initio methods. It is hoped that the results found in this work will serve as a reference for future experimental and theoretical studies of this compound.

#### REFERENCES

- [1] Nowotny, H., Funk, R., Pesl, J., Monatshefte für chemie und verwandte Teilie anderer Wissenschaften. **82**, 3 (1951) 513-525.
- [2] Failamani, F., Broz, P., Maccio, D., Pchegger, S., Müller, H., Salamakha, L., Michor, H., Grytsiv, A., Saccone, A., Bauer, E., Rogl, P., J. Intermetallics. **65** (2015) 94-110.
- [3] M. Armbrüster, "Bindungsmodelle für intermetallische Verbindungen mit der Struktur des CuAl<sub>2</sub>-Typs," Cuvillier Verlag, (2005) 111.
- [4] Schwarz, K., Blaha, P., Solid state calculations using WIEN2k. Computational Materials Science. **28**, 2 (2003) 259-273.
- [5] Madsen, G & Singh, D, J. BoltzTraP, A code for calculating band-structure dependent quantities. Computer Physics Communications. **175**, 1 (2006) 67-71.
- [6] Larcher, D., Beaulieu, L. Y., Mao, O., George, A. E., Dahn, J. R., J. The Electrochemical Society. **147**, 5 (2000) 1703-1708.
- [7] Li, X, H., Cui, H, L & Zhang, R. Z. Mechanical, acoustical, and optical properties of several Li-Si alloys: a first-principles study. Journal of Zhejiang University Science A. **20**, 8 (2019) 614-626.
- [8] Sakhaya, A. P., Dutta, A., Shannigrahi, S. & Sinha, T.P. Electronic structure and optical properties of orthorhombic RAlO<sub>3</sub> (R=Sm, Nd). Solid State Sciences. **42** (2015) 37-44.
- [9] Bilokur, M., Gentle, A., Arnold, M., Optical properties of refractory TiN, AlN and (Ti, Al) N coatings. In: Micro+ Nano Materials, Devices, and Systems. International Society for Optics and Photonics. **9668** (2015) 966850.
- [10] Koutsokeras, L. A., Abadias, G., Lekka, C. E., Matenoglou, G. M., Anagnostopoulos, D. F., Evangelakis, G. A & Patsalas, P. Conducting transition metal nitride thin films with tailored cell sizes: The case of  $\delta$ -Ti<sub>x</sub>Ta<sub>1-x</sub>N. Applied Physics Letters. **93**, 1 (2008) 011904
- [11] Yazami. R. Nanomaterials for Lithium-ion batteries: Fundamentals and Applications. Jenny Stanford Publishing, (2013).

- [12] Schwarz, K. DFT calculations of solids with LAPW and WIEN2k. *Journal of Solid State Chemistry*. **176**, 2 (2003) 319-328.
- [13] P. Blaha, "Wien2k, An Augmented Plane Wave Plus Local Orbitals Program for Calculating Crystal Properties," (2001).
- [14] Engel, E., Vosko S H. *J. Physical Review B*. **47**, 20 (1993) 13164.
- [15] Malki, S., El Farh, L., *J. Materials today: proceeding*. **13**, 3 (2019) 991-997.
- [16] Armbrüster, M., Schnelle, W., Schwarz, U., Grin, Y.J. *Inorganic Chemistry*. **46**, 16 (2007) 6319-6328.
- [17] Jepsen, O & Andersen O. K. The Stuttgart TB-LMTO Program. Max-Planck-Institut für Festkörperforschung: Stuttgart, Germany, (1998).
- [18] Schwarz, K, Blaha, P, Madsen, G.K.H. *Electronic Structure Calculations of Solids Using the WIEN2k package for Material Sciences. Comput. Phys. Commun.* **147**, 1-2 (2002) 71-76.
- [19] M. S. Dresselhaus, "Solid state physics part II optical properties of solids," (2001) 6-7.
- [20] Ehrenreich, H. *The optical properties of metals, IEEE spectrum*. **2**, 3 (1965) 162-170.
- [21] Monkhorst, H. J., Pack, J. D., *J. Physical Review B*. **13**, 12 (1976) 5188.
- [22] Bakhshayeshi, A., Sarmazdeh, M. M., Mendi, R. T., Bouchani, A., *J. Electronic Materials*. **46**, 4 (2017) 2196-2204.
- [23] M. M. Noskov, "Optical and Magneto-optical Properties of Metals," Sverdlovsk: UNTS, (1983) 217.
- [24] Khan, S. A., Reshak, A. H., Alahmed Z A., *J. Materials science*. **49**, 14 (2014) 5208-5217.
- [25] Solli, D., Chia, R. Y., Hickmann J. M., *J. Physical Review E*. **66**, 5 (2002) 056601.
- [26] Ding, An H., Ya-Guang, Z., Wei-Cheng, C., Shao-Guang, D., Chun-Qing, H., Chuan-Yun, Z., Pei-Ying, L., *J. Communications in Theoretical Physics*. **55**, 4 (2011) 671.
- [27] F. Wooten, "Optical properties of solids," Academic Press, New York, (1972) 28.
- [28] Monir, M. E. A., Baltache, H., Khenata, R., Murtaza, G., Mahmood A., *J. Superconductivity and novel magnetism*. **29**, 5, (2016) 1255-1266.
- [29] Anjami, A., Bouchani A., Elahi, S.M., Akbari H., *J. Results in physics*. **7** (2017) 3522-3529.
- [30] Olmon, R. L., Slovick, B., Johnson, T.W., Shelton, D., Oh, S H., Boreman, G D., Rachke, M B., *J. Physical Review B*. **86**, 23 (2012) 235147.
- [31] Ramanna, J., Yedukondalu, N., Babu, K. R., Vaitheeswaran, G., *J. Solid State Sciences*. **20** (2013) 120-126.
- [32] M. Dressel, G. Gruner, "Electrodynamics of Solids," Cambridge University Press, Cambridge, UK, (2002) 208-209.
- [33] F. A. Han, "Modern course in the quantum theory of solids". World Scientific, (2013) 507.
- [34] Muhammad, N., Khan, A., Khan, S. H., Siraj, M. S., Shah, S. S. A., Murtaza, G., *J. Physica B: Condensed Matter*. **521** (2017) 62-68.